JACS
JOURNAL OF THE AMERICAN CHEMICAL SOCIETY
pubs.acs.org/JACS
Article

Ligand Desorption and Fragmentation in Oleate-Capped CdSe Nanocrystals under High-Intensity Photoexcitation

Samantha M. Harvey, Jacob H. Olshansky, Alice Li, Shobhana Panuganti, Mercouri G. Kanatzidis, Joseph T. Hupp, Michael R. Wasielewski, and Richard D. Schaller*

Cite This: https://doi.org/10.1021/jacs.3c10232
Read Online

ABSTRACT: Semiconductor nanocrystals (NCs) offer prospective use as active optical elements in photovoltaics, light-emitting diodes, lasers, and photocatalysts due to their tunable optical absorption and emission properties, high stability, and scalable solution processing, as well as compatibility with additive manufacturing routes. Over the course of experiments, during device fabrication, or while in use commercially, these materials are often subjected to intense or prolonged electronic excitation and high carrier densities. The influence of such conditions on ligand integrity and binding remains underexplored. Here, we expose CdSe NCs to laser excitation and monitor changes in oleic acid that is covalently attached to the NC surface using nuclear magnetic resonance as a function of time and laser intensity. Higher photon doses cause increased rates of ligand loss from the particles, with upward of 50% total ligand desorption measured for the longest, most intense excitation. Surprisingly, for a range of excitation intensities, fragmentation of the oleic acid is detected and occurs concomitantly with formation of aldehydes, terminal alkenes, H_2, and water. After illumination, NC size, shape, and bandgap remain constant although low-energy absorption features (Urbach tails) develop in some samples, indicating formation of substantial trap states. The observed reaction chemistry, which here occurs with low photon to chemical conversion efficiency, suggests that ligand reactivity may require examination for improved NC dispersion stability but can also be manipulated to yield desired photocatalytically accessed chemical species.

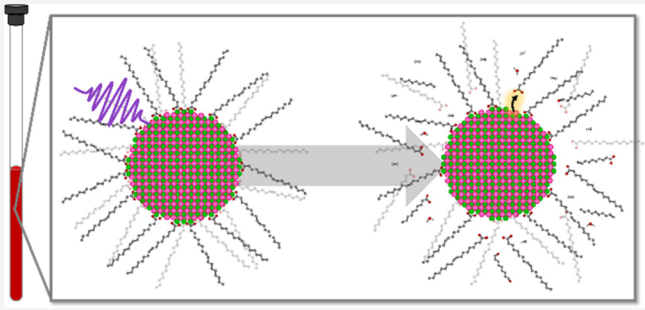

■ INTRODUCTION

Colloidal semiconductor nanocrystals (NCs) are heralded for their desirable photophysical properties (e.g., large absorption cross sections, visible, and near-infrared absorption, narrow emission) that are tunable through size and morphology in addition to composition.[1] These materials typically present 1−10 nm inorganic crystalline core size and long-chain alkyl ligand surface termination.[2] Ligands are critical not only for colloidal stability but also for passivating the undercoordinated surfaces of NCs to promote radiative recombination rather than surface trapping.[3] The coupling of the optoelectronic properties produced by the semiconductor core with robust syntheses and solution processability bolstered by capping ligands have led to semiconductor NC implementation for a wide range of applications including photocatalysis,[4−6] photovoltaics,[7−9] display technologies,[10,11] biosensing,[12] and lasing.[13,14]

Many of the features of NCs that make them desirable for applications bring complications, as well. Quantum confinement of carriers permits tunability of absorption and emission, yet also gives rise to rapid Auger recombination of multiexcitons that can cause substantial heating rather than light output.[15] Colloidal suspensions offer compatibility with dropcasting, spin-coating, or printing as inks,[16,17] but the interface between the semiconductor lattice and the ligands/surrounding media impacts heat dissipation.[18,19] This coupled with reduced melting temperatures due to high surface energies compared to bulk bonding can prove problematic for high-intensity excitation applications such as solar concentrators, lasers, and LEDs.[19,20] The high surface areas of NCs are not only promising as catalytic sites but are also prone to oxidation, especially if in conditions that cause excess charges to remain.[21−23] While some applications (e.g., photonic curing,[24,25] photothermal therapy[26]) aim to use such properties of NCs to their benefit, most are hindered by them. Despite understanding that excitation may negatively impact NCs, a comprehensive microscopic picture of sample evolution under the relevant conditions is lacking. Even in laboratory settings, when NCs are excited to study their

Received: September 17, 2023
Revised: January 7, 2024
Accepted: January 9, 2024

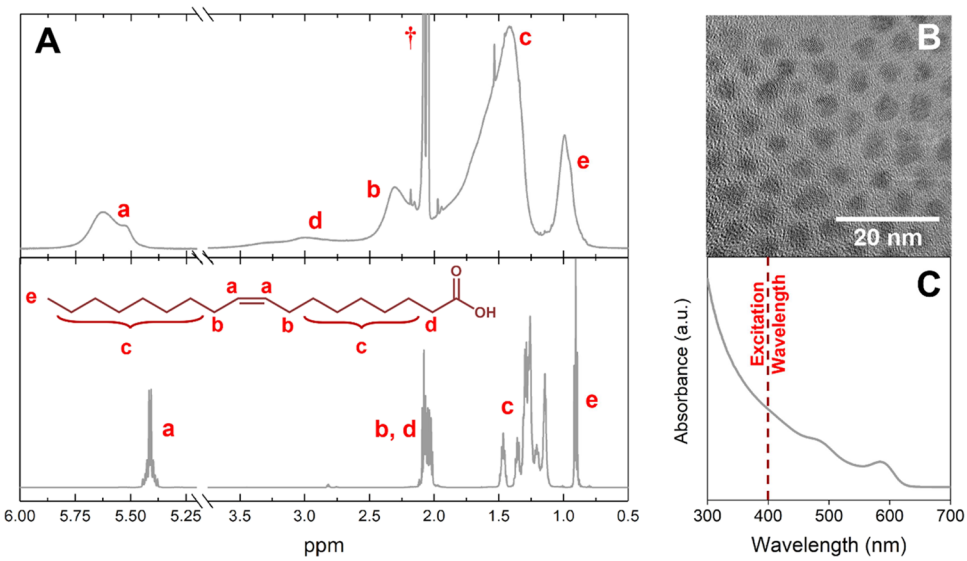

Figure 1. CdSe NCs before photoexcitation. (A) NMR spectra of oleate-terminated CdSe NCs (top) and oleic acid free in solution (bottom). Protons are assigned for each; residual toluene is labeled with †. (B) TEM image of the NCs. Diameter was measured to be 4.2 ± 0.8 nm. (C) Absorption spectrum of as-synthesized particles with the excitation wavelength (400 nm) is marked.

optoelectronic behavior, there is little systematic study and understanding related to the effects of laser pumping over the course of optical measurements. Oftentimes NCs that have exhibited these behaviors are discarded without further probing to uncover *what* is occurring and *why* because they are considered "dead" optically, their photoluminescence has dropped substantially, or precipitation renders them challenging or impossible to colloidally process further.

The understanding of photophysical properties in semiconductor NCs has advanced significantly, but only recently research has begun to delve deeply into NC degradation. Many studies focus purely on detrimental effects pertaining to the crystalline lattice; monitoring structural changes or as optical characteristics diminish, yet the surfaces and ligand shell are critical components of colloidal NCs that merit in-depth study. This is especially true given that surface oxidation, particle charging, and ligand loss are inherently tied to each other as well as a major contributor to carrier trapping that limits photoluminescence quantum yield.[27,28] Above-gap optical excitation of a NC can potentially liberate surface ligands owing to electrical charge movement to the interface that might disrupt bonding from chemical conversions of the interfacial species, or if not at equilibrium, from increased resultant thermal energy that promotes desorption.[29,30] If ligands desorb or chemically change in sufficient numbers, colloidal NC dispersions that initially were stable can aggregate as attractions provided by van der Waals forces become stronger with reduced average NC−NC separation. Additionally, the particles may become charged or their surfaces oxidized, resulting in increases in carrier trapping that limit radiative recombination. Hollingsworth and co-workers have examined how photoexcitation can reduce photoluminescence lifetime through thermal and oxidative surface degradation, effectively "killing" a NC.[31,32] Shulenberger et al. showed that continuous wave (CW) illumination of CdS NCs resulted in particle charging by monitoring changes in the absorption spectra.[30] While these studies have contributed to a fuller picture of how photoexcitation impacts the entire structure of NCs, they do not directly probe ligand behavior. To the best of our knowledge, no studies have correlated how photoexcitation of the inorganic core might directly impact the organic ligands, an important step toward understanding changes to NC photophysics.

Toward this goal, we investigate oleate-terminated CdSe NCs under pulsed laser illumination as a function of light intensity and total exposure. We utilize nuclear magnetic resonance (NMR) spectroscopy as our primary technique for monitoring ligand evolution as it is noninvasive and allows quantitative measurement of molecular species.[33] Importantly, NMR can differentiate between different molecular species and probe whether such species are bound to the surface of the NC or not via chemical shift and peak broadening. By comparing the same NC sample under different conditions, we find both that ligands irreversibly detach from the NC surface over the course of optical exposure and observe increased unbound ligand as denoted by changes in resonance and line shape. Unexpectedly, we also note appreciable chemical changes to these ligands upon light exposure; ligand degradation products and small molecules, including aldehydes, water, and molecular hydrogen, form in nearly all experiments. In conjunction with transmission electron microscopy (TEM), X-ray diffraction (XRD), and photoluminescence, a range of properties are investigated, from fusing/sintering of NCs to photobrightening and eventually substantial decreases in photoluminescence intensity. Whereas the lowest-energy absorption feature persists with exposure, Urbach tails, consistent with increasingly poorly passivated surfaces, appear commensurate with appreciable ligand loss. This study serves as a first look into photoinduced changes in CdSe NCs passivated by oleate and aims to address some of the questions raised above while providing promising future directions.

■ RESULTS AND DISCUSSION

Oleate-terminated CdSe NCs were synthesized following existing protocols described in the Supporting Information (SI).[34] Particles were cleaned via three rounds of centrifugation with isopropyl alcohol and methanol as antisolvents. ^{1}H NMR was used to confirm the ligand identity as well as the

https://doi.org/10.1021/jacs.3c10232
J. Am. Chem. Soc. XXXX, XXX, XXX−XXX

Table 1. Photophysical Properties and Diameter of CdSe NCs before and after Photoexcitation

sample	laser power and spot size	$\langle N \rangle$	photoexposure times (min)	abs. max (nm)	PL max (nm)	diameter (nm)	$\langle \tau \rangle_{PL,5ns}$ (ns)	$\langle \tau \rangle_{PL,50\ ns}$ (ns)
control				585	598	4.19 ± 0.81	4.9 ± 0.3	7.4 ± 0.4
Tube 1	140 mW, 9.8 mm^2	4.2	30, 90, 150	583	599	4.19 ± 0.71	6.1 ± 0.5	8.3 ± 0.3
Tube 2	140 mW, 0.85 mm^2	49	15, 30, 60, 85	583	599	4.19 ± 0.75	4.6 ± 0.5	7.4 ± 0.4
Tube 3	140 mW, 0.071 mm^2	584	15, 30, 60, 85	580	603	4.36 ± 0.83	1.6 ± 0.1	3.1 ± 0.3
Tube 4	75 mW, 0.071 mm^2	313	15, 30	583	599	4.28 ± 0.79	4.4 ± 0.5	6.8 ± 0.3

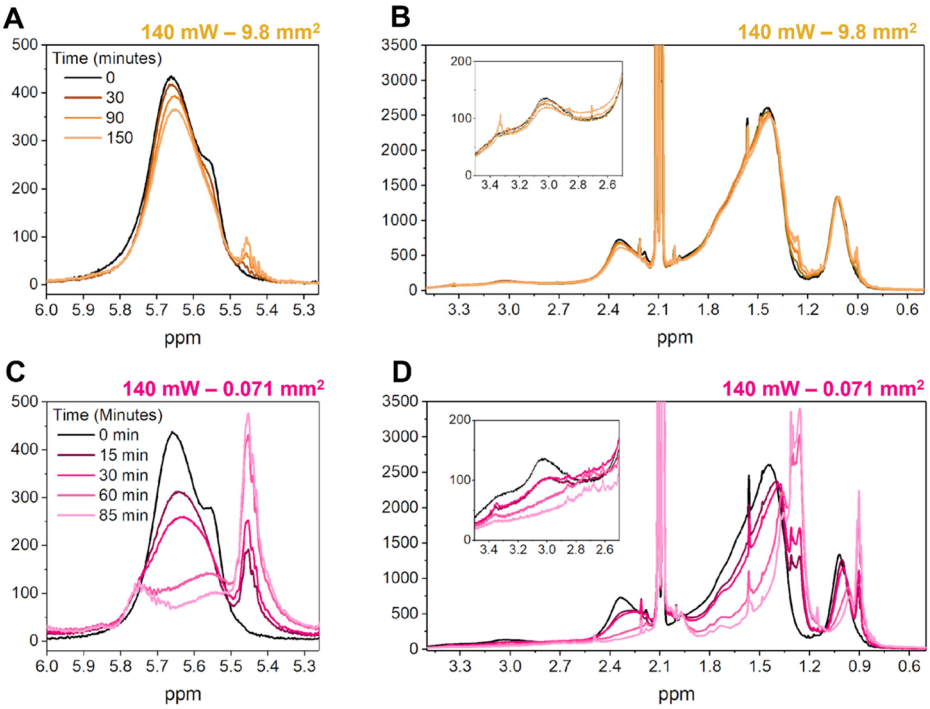

Figure 2. Photoinduced ligand desorption. NMR spectra of Tubes 1 (A, B) and 3 (C, D) as a function of laser exposure time.

successful removal of any unbound molecular species. Figure 1A shows NMR spectra of the NCs compared to those of oleic acid in deuterated toluene. As expected, the proton features of bound oleate are broadened and shifted downfield, compared to free oleic acid, due to reduced diffusion-altering relaxation times.[33] Peaks are marked with the corresponding proton assignments. Importantly, vinylic protons, which appear near 5.6 ppm (marked by **a**), are broad and lack sharp features that would otherwise correspond to unbound oleic acid at around 5.4 ppm. Throughout this study, we focus on this region as it is less congested by alkyl or aromatic proton signals, allowing ease of fitting and analysis. TEM and absorption measurements (Figure 1B,C) show a monodisperse sample with a diameter of 4.2 ± 0.8 nm and a distinct lowest energy peak at 585 nm.

To ensure a direct comparison, the CdSe NC sample described above was used for all experiments appearing in this report. The sample was separated into six aliquots and examined under a range of different conditions. Aliquot samples 1−4 were illuminated at 400 nm using a 1 kHz pulsed, 100 fs pulsewidth laser. The samples, contained in NMR tubes, were mechanically rastered such that the entirety of the sample volume was illuminated over the course of the experiments. Incident power on the NC dispersions was adjusted using a neutral density wheel, and laser spot size was controlled using an iris and altered focal distance. For samples 1−3, the average laser power was maintained at 140 mW, but the spot size was adjusted to 9.8, 0.85, or 0.071 mm^2, respectively. This results in a constant number of incident photons but altered fluence which changes the number of photons absorbed per particle per pulse. Tube 1 experienced 1.43 mJ/cm^2 resulting in an average number of excitons ($\langle N \rangle$) per NC of 4.2, Tube 2 experienced a fluence of 16.5 mJ/cm^2 giving $\langle N \rangle$ = 49, and Tube 3 experienced 197 mJ/cm^2 giving $\langle N \rangle$ = 584. Tube 4 was exposed to half the laser power of the other samples (75 mW) but the same spot size as 3, resulting in a fluence of 106 mJ/cm^2 and $\langle N \rangle$ = 313. Throughout the experiment, photoexcitation was paused at set time points so that NMR spectra could be recorded. All other characterization was preformed after the final light dosing. While excitation regimes examined in this work in some cases exceed those of usual device-relevant ranges, they are in line with those of photonic curing and optical amplification and were chosen to ensure that we could draw meaningful conclusions about the dependencies and mechanisms of ligand desorption and fragmentation.[14,24]

The last two samples, Tubes 5 and 6, were not photoexcited. One was maintained as a control for all measurements, with the only modification being the addition of CH_2Br_2 as an internal standard for determining ligand density (see SI for calculation). Based on this internal calibrant, as synthesized, the CdSe NCs have ∼3.4 molecules/nm^2 which is consistent with multiple reports.[35−38] The latter sample, Tube 6, was flame-sealed for variable temperature experiments without laser illumination to evaluate the thermal dissociation of ligands. A summary of all samples is provided in Table 1.

https://doi.org/10.1021/jacs.3c10232
J. Am. Chem. Soc. XXXX, XXX, XXX−XXX

NMR spectra collected for Tubes 1 and 3 are displayed in Figure 2A–D. Over the course of increasing laser exposure time, ligands increasingly dissociate from the surfaces of the NCs as indicated by the appearance of sharp (unbound ligand) NMR peaks around 5.4 ppm and the reduction of the broad (bound) 5.6 ppm peak. The alkyl features also shift upfield and sharpen due to desorption. To quantitatively determine the extent of ligand loss, fitted peak areas in the range of 5.3–6 ppm were separated into "bound" or "free" depending on chemical shift and width (Figure S11). The percentage of free ligand versus time for Tubes 1–4 are given in Figure 3A.

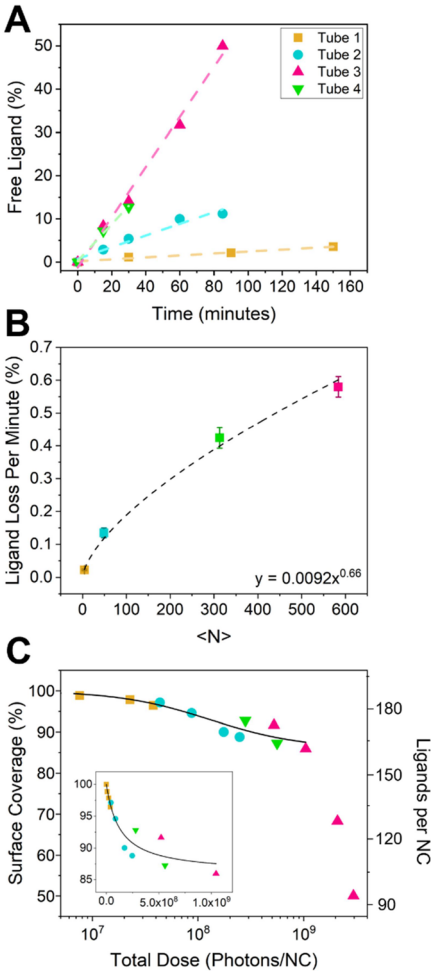

Figure 3. Ligand loss over the course of experiments. (A) Ratio of integrated free ligand signal versus total ligand for the four photoexcited samples. Linear fits for each laser fluence as a function of time provide rates for ligand loss. These rates are plotted against ⟨*N*⟩ in (B) where a nonlinear response is noted by fit to a power function. (C) Total absorbed photons per NC versus surface coverage fit to a Langmuir isotherm.

Although ligand loss is linear with the number of photons absorbed, Tubes 1–3 do not show the same slope, suggesting the process for desorption is dependent on the density of photons. As the fluence is increased (by decreasing spot size), more ligands are dissociated from the surface with upward of ∼50% desorption from Tube 3 after 85 min of illumination versus ∼3% desorption with the same total number of photons but with lower intensity in Tube 1. The NCs remained stable in solution with no aggregation evident over the course of the experiments. Given months in solution, NCs in Tube 3 did experience loss of colloidal stability as noted by precipitation, whereas the other tubes that showed less ligand loss in total did not. Tube 4 showed similar ligand loss to Tube 3 despite approximately half the incident power (and therefore half the absorbed photon dose) suggesting a ⟨*N*⟩ threshold above which continued photon absorption does not result in ligand loss. Once dissociated, ligands did not readsorb onto the surface of the NCs with time, suggesting an irreversible change. Such a process, even if low in terms of quantum yield, thus can be important for NC implementation.

Desorbed ligand amount (relative to initial ligand coverage) appears linear versus exposure time in each case, and linear fits provide a rate of ligand loss per minute relative to ⟨*N*⟩. As we describe above, this rate does not increase linearly with ⟨*N*⟩, but instead it seems to approach a maximum rate of ligand loss upon which higher fluences yield similar results (Figure 3B). This allows us to approximate the length of time required for an arbitrary percentage of ligand dissociation at low ⟨*N*⟩. For example, at an ⟨*N*⟩ value of 0.05, to achieve 1% ligand loss would require ∼13 h and 50% ligand loss would require over 27 days of the described laser exposure.

Mechanistically, thermal energy may play a key role in the observed ligand desorption, where optical excitation produces phonons through intraband relaxation and Auger recombination. For the system to return to equilibrium, this heat must be dissipated through the particle, interface, and ligands, potentially causing release of bound surface species. To determine whether static heating from laser illumination could cause ligand desorption, we performed variable temperature NMR to monitor changes in the population of bound and free ligand upon heating to 100 °C. We were limited to this temperature range due to the boiling point of d8-toluene, but assume that prolonged exposure at 100 °C could promote desorption given literature precedence for photogenerated temperature increases and that the lowest pulsed excitation regime studied here experienced ligand loss after only 15 min.[19,39−41] With sample temperature elevation, ligand loss was not observed, and even after maintaining the sample at 100 °C for 1 h, no solvated oleic acid features were detectable (Figure S25). These results are consistent with other heating experiments in the literature.[42] We do note, however, that the shoulder present on the downfield side of the vinylic proton feature decreases concurrently with the increased intensity of the main peak. This is potentially due to the rearrangement of ligands on the surface into more energetically favorable configurations, suggestive of some form of sample surface or ligand annealing. Reports on InP NCs have shown that these two features can be correlated to edge and facet binding site, further evidence of ligand migration or loss of higher energy edges.[43] In the photoexcited samples, desorption of ligands tends to deplete this shoulder first, as well. Regardless, the absence of thermally induced ligand dissociation over this accessible temperature range suggests photoexcitation may be producing even higher temperatures (resulting in surface melting) or that carriers lead to chemical changes of the NC surface or ligands.

While our focus here was on pulsed excitation, we also illuminated a sample of CdSe NCs with above-band gap CW illumination with an average power of 140 mW and intensity of approximately 580 mW/cm^2 (Figure S27). We saw no discernible ligand loss after 75 min under these conditions with similar number of total absorbed photons to pulsed measurements. Given that CW excitation results in a lower ⟨*N*⟩

https://doi.org/10.1021/jacs.3c10232
J. Am. Chem. Soc. XXXX, XXX, XXX−XXX

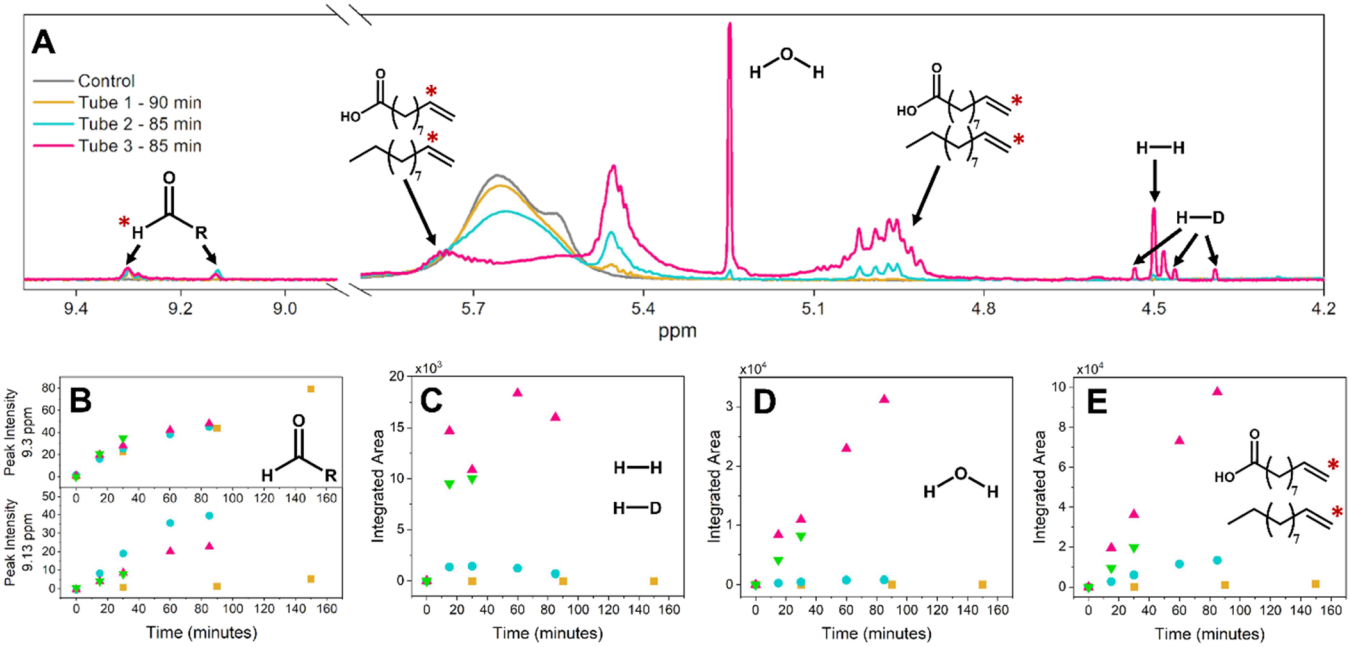

Figure 4. Ligand fragmentation. (A) Tubes 1−3 after similar photoexcitation dose times. Chemical shifts of new molecular species that arise from fragmentation of the oleic acid ligand or reaction with toluene are marked by red asterisks (*). (B−E) Chemical species as a function of laser exposure time. (B) Aldehyde features at 9.13 and 9.3 ppm, (C) hydrogen features between 4.4 and 4.55 ppm, (D) water clusters peak at 5.25 ppm, and (E) terminal protons of undecane or undecanoic acid between 4.9 and 5.1 ppm.

than pulsed, we are in a regime where the vast majority of NCs have one or no excitons suggesting that Auger processes, multiphoton absorption, or ionization may be critical to ligand loss. It is important to note that higher intensity CW fluences have produced ligand loss and are accessed in LED and photocatalysis experiments.[31,32,44,45]

Conversion of the collected data from Figure 3A to photons/NC provides a measure of the total absorbed dose across the four samples (Figure 3C). When plotted in this manner, ligand loss percentage appears to follow a trend between samples, with increasing desorption occurring as photon flux increases. We were able to fit most of the data plotted in this way to a Langmuir binding isotherm (eq 1) where θ is the fraction of free ligand, K_d is the dissociation constant, $[h\nu]$ is the total absorbed dose, and constant a relates saturation. This model was chosen as it is commonly used to describe ligand binding and desorption from NC surfaces.[42,46] As far as we are aware, this is always studied with the addition of a competing ligand that induces exchange instead of photoexcitation; however, there are examples of Langmuir isotherms applied to photoreactions in biological systems.[47] Ligand desorption values above ∼14% cease to follow a simple Langmuir model and were excluded from the fit.

$$\theta = \frac{aK_d[h\nu]}{1 + K_d[h\nu]} \tag{1}$$

We find that the dissociation constant (K_d) is 7.7×10^{-9} NCs/photons for this binding isotherm. Given that each NC initially has ∼188 ligands, this translates into $K_d = 1.5 \times 10^{-6}$ ligands/photon. This low quantum yield is consistent with our need for pulsed laser excitation and a lack of appreciable ligand loss with low-power CW illumination. While we were unable to fit to a two isotherm model, curiously, the data fit well to a biphasic equation that is commonly used to describe two binding sites (e.g., observed in bimodal drug release, see SI for more information).[48] The need for two phases once again suggests a difference in the binding motif or binding strength. This could correspond to differences in binding modes (bidentate versus monodentate, edge versus facet), a change in ligand displacement type (X-type oleic acid versus Z-type Cd-oleate), or suggests that a fundamentally different process occurs at particularly high fluences.[42,49] At this time, we are unable to resolve the species from our data that constitute the two different binding motifs. As mentioned above, we do observe loss of the upfield shoulder on the vinylic protons, which could be due to differences in faceting as reported for InP; however, we cannot be certain that such behavior is at play with our particles as they are spheroidal. Furthermore, we are unable to distinguish between liberated oleic acid and Cd-oleate due to the similarity in chemical shift. This biphasic model provides an upper limit for ligand dissociation of 60 ± 10%, suggesting that above this point NCs either do not lose any more ligand or further ligand loss results in colloidal instability. Precipitation of such particles would prohibit their involvement in NMR signals, i.e., they would become invisible to the techniques used here, but precipitate was not observed for the range of parameters studied herein.

In addition to ligand loss, NMR resonances develop that cannot be attributed to oleic acid but instead clearly indicate formation of new chemical species as shown in Figure 4. At 4.9−5.05 and 5.65−5.8 ppm, clear signatures of the vinylic hydrogens of undecane or undecanoic acid are evident.[50] We are not able to distinguish between these chemical species given the similarity in their proton shifts, but integration confirms their identity. In addition, a strong feature at 5.25 ppm grows in that corresponds to water. Given the nonpolar nature of toluene, any water formed produces clusters that yield a distinctive chemical shift.[51,52] Around 4.3 ppm, sharp peaks demarking molecular hydrogen (H_2, HD) are present.[53] Indeed, in some experiments, bubbles were clearly observed to

https://doi.org/10.1021/jacs.3c10232
J. Am. Chem. Soc. XXXX, XXX, XXX−XXX

form in the tube consistent with this assignment (although we note that CO_2 is also a possible side product that would not appear in ^{1}H NMR). Furthermore, the integrated peak area for these features is relatively constant, suggesting formation of dissolved gases that eventually leave the solution. Given that HD is present alongside H_2 (Figure S13) chemical interaction between the deuterated toluene and the NCs must be occurring, suggesting radical formation. Cadmium chalcogenide NCs have been shown to be viable hydrogen evolution catalysts using formic acid or water.[54,55] Features around 9 ppm demarcate aldehyde protons, although again we cannot be quite clear as to molecule identity. Aldehydes can form upon the loss of the hydroxide group from oleic acid or oxygen addition to the double bond. Two distinct features in this region show different behaviors with photoexcitation. The peak at ~9.3 ppm forms on similar time scales of illumination regardless of the range of fluences studied. The peak at 9.13 ppm, however, shows behavior more similar to the other chemical species and ligand desorption (i.e., fluence dependent). As oleic acid will only readily exchange on the surfaces of CdSe NCs in the presence of a proton source, this fragmentation may be further enabling ligand dissociation.[56]

We note that no chemicals were added to these samples to cause fragmentation. The NMR spectrum of our oleic acid showed no evidence of these chemical species, nor were they present in the NC spectrum before photoexcitation. As a control experiment to determine if the CdSe NCs were necessary for this oleic acid degradation process, we illuminated a tube of concentrated oleic acid in deuterated toluene using a higher fluence than the other tubes for a longer length of time as described in Figure S24. Even with these more intense, more sustained excitation conditions, only trace amounts of undecane/undecanoic acid and aldehydes were seen and neither hydrogen nor water were observed. Along with the temperature-dependent NMR, this control measurement suggests that a combination of laser irradiation, CdSe, and oleate is necessary to generate the observed photoproducts.

One might expect an appreciable morphological evolution of NC dispersions upon intense, sustained laser exposure in solution. However, TEM images of the NCs after photoexcitation reveal particle shape and size remain largely unchanged for the range of fluences and exposure times examined (Figure 5A–D). NCs exposed to the highest intensity (Sample 3) experienced trace amounts of sintering between some NCs to form larger agglomerated structures (~8–10 nm). Given that distinct crystallographic domains can be seen within these larger NCs (see Figure S4 for more examples), we suggest that ligand loss likely produces colloidal instability and increases close contact of NC surfaces. Samples 1 and 2 showed no discernible difference in NC diameter, and rather a slight narrowing in distribution, consistent with laser annealing. Powder XRD measurements indicate that the materials persist in the initial zincblende crystalline phase (Figure 5E). Broadening of diffraction peaks in Tube 3 suggests smaller crystalline domains have formed, consistent with loss of surface layers and ligands that lead to agglomeration. Scherrer analysis shows a reduction in crystallite size of approximately 0.6 nm in Tube 3, but the remaining samples were unaffected (Figure S9).

Optical properties offer additional information regarding the impact of exposure and ligand loss, which is crucial regarding the performance in optoelectronic devices. UV–vis shows that

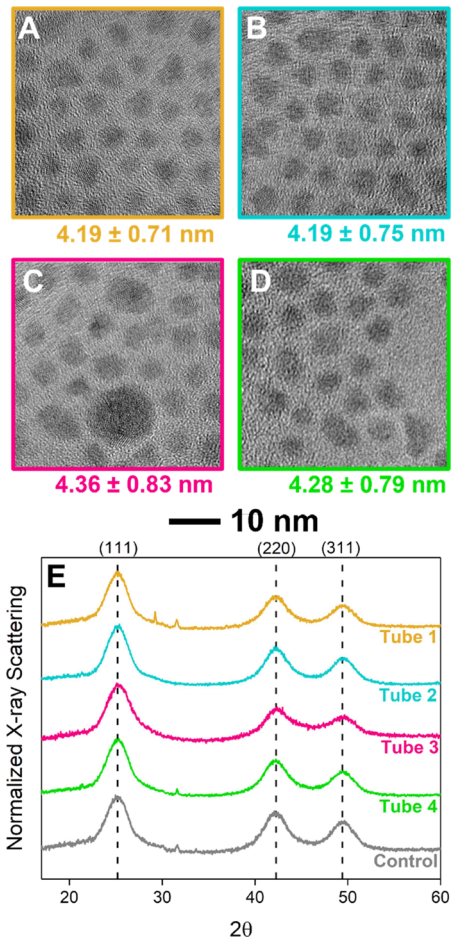

Figure 5. Characterization of the samples after photoexposure. (A–D) TEM images of Tubes 1–4 and the corresponding diameters measured. (E) XRD patterns of Tubes 1–4 and the control.

the absorption has only slightly shifted by just 2–5 nm (see Table 1) although Sample 3, and to a lesser extent Sample 4, shows a broadening of features and emergence of a tail to the red. This absorption is lower in energy than bulk CdSe (marked by the dashed line at 713 nm), and we attribute this feature to trap state formation within the bandgap (an Urbach tail).[27] Low concentrations and solvent correction were used to ensure that this was not an artifact of scattering. As noted above, despite ligand loss, all samples showed no precipitation initially.

Static and time-resolved photoluminescence (Figure 6B,C) provides further insight into the impacts of surface passivation. Despite broadening and the appearance of midgap trap states observed by absorption, no emission red of the main band-edge feature is observed, though Sample 3 did exhibit broadening and a slight red shift of PL. All samples maintained a similar emission wavelength, consistent with the bandgap and particle size remaining close to the control. We find that Samples 1 and 2 showed brightening after ligand loss suggesting a reduction of trap states either through annealing of intrinsic defects or reorganization of ligands into a position or binding motif that is more favorable for radiative recombination. Other reports of photobrightening have also attributed changes to surface oxidation states through ligand loss.[31,32,57,58] Sample 3 showed a drastic reduction in emission intensity, likely due to formation of numerous trap sites. We

https://doi.org/10.1021/jacs.3c10232
J. Am. Chem. Soc. XXXX, XXX, XXX−XXX

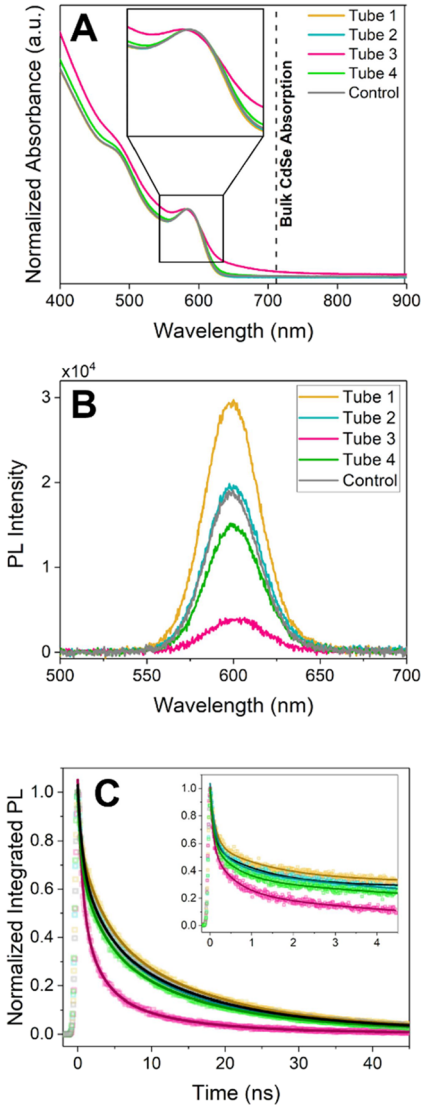

Figure 6. Optical characterization of samples after prolonged illumination. (A) Absorption spectra for photoexcited samples and the control. Inset shows the lowest energy absorption in finer detail. Bulk CdSe absorption at 713 nm is given as a dashed line. (B) Static PL spectra. (C) Time-resolved PL spectra over 50 and 5 ns (inset) along with triexponential fits.

observed similar results via time-resolved measurements using a streak camera to spectrally and temporally resolve the PL. No evidence of trap state emission at redder wavelengths was found although some increase in blue emission (<550 nm) appeared in Tube 3. Integration of PL from 525 to 675 nm provides emission dynamics shown in Figure 6C, which were fit to multiexponentials to provide the average PL lifetimes $\langle\tau\rangle$ listed in Table 1. Tube 1 exhibited longer lifetimes, while Tube 3 showed a more substantial reduction in lifetimes. Such observations again are consistent with large trap populations for the highest pump intensity and possible annealing for the lower intensity exposures. Similarities in early time dynamics with drop in emission at later times are consistent with reports of charging.[32]

■ CONCLUSIONS

In this work, we have demonstrated that photoexcitation of oleate-capped CdSe NCs results in irreversible ligand loss as a function of exposure time and pump intensity. The rate of ligand desorption correlates with laser fluence and, in the extreme, upward of 50% of ligands are removed after 85 min at 197 mJ/cm^2. From these results, we calculated a rate of ligand loss per photons absorbed of 1.5×10^{-6}. While this low quantum yield may not appreciably affect NCs under standard illumination, photon density in high-intensity CW and pulsed conditions is enough to irreversibly desorb ligands from the surface and produce chemical changes. In addition to ligand loss, fragmentation of oleate resulted in formation of water, molecular hydrogen, undecane/undecanoic acid, and aldehydes as evident by NMR. All NC samples maintain the zincblende structure, and size is unaffected except at the highest fluence which resulted in minor particle sintering after ligand loss. Absorption and emission profiles were largely maintained although PL intensity showed photobrightening in the lower fluence samples and a sharp reduction for the highest fluence sample further suggesting surface rearrangement and trap formation under such conditions of significant ligand degradation and desorption. These results have implications for NC and ligand stability in a wide range of applications that depend on high-intensity illumination including solar concentrators, LEDs, lasers, and photocatalysts. Beyond concerns about the stability of the inorganic core (e.g., photobleaching, charging), ligand fragmentation is of particular concern given that the chemical processes likely remain active even in solid-state devices, whereas ligand desorption potentially decreases in the solid state as diffusion of desorbed ligand would be impeded. Influence of colloidal dispersion versus solid-state conditions will be examined in future studies. We hope this work serves as a preliminary exploration into the effects of light-induced ligand and surface restructuring in semiconductor NCs.

■ ASSOCIATED CONTENT

Supporting Information

The Supporting Information is available free of charge at https://pubs.acs.org/doi/10.1021/jacs.3c10232.

Experimental methods and supplementary data, synthesis of CdSe NCs, quantification of NC and ligand concentration, photon density calculations, TEM images, Scherrer analysis of XRD data, NMR fits and analysis, additional photoluminescence data, and control experiments (PDF)

■ AUTHOR INFORMATION

Corresponding Author

Richard D. Schaller − *Department of Chemistry and International Institute for Nanotechnology, Institute for Sustainability and Energy at Northwestern, Northwestern University, Evanston, Illinois 60208, United States; Center for Nanoscale Materials, Argonne National Laboratory, Lemont, Illinois 60439, United States;* orcid.org/0000-0001-9696-8830; Email: schaller@northwestern.edu, schaller@anl.gov

Authors

Samantha M. Harvey − *Department of Chemistry and International Institute for Nanotechnology, Institute for Sustainability and Energy at Northwestern, Northwestern University, Evanston, Illinois 60208, United States*

Jacob H. Olshansky − *Department of Chemistry and International Institute for Nanotechnology, Institute for Sustainability and Energy at Northwestern, Northwestern University, Evanston, Illinois 60208, United States;* orcid.org/0000-0003-3658-1487

Alice Li − *Department of Chemistry, Northwestern University, Evanston, Illinois 60208, United States;* orcid.org/0000-0003-0667-2118

Shobhana Panuganti − *Department of Chemistry, Northwestern University, Evanston, Illinois 60208, United States;* orcid.org/0000-0003-1762-527X

Mercouri G. Kanatzidis − *Department of Chemistry and International Institute for Nanotechnology, Institute for Sustainability and Energy at Northwestern, Northwestern University, Evanston, Illinois 60208, United States;* orcid.org/0000-0003-2037-4168

Joseph T. Hupp − *Department of Chemistry and International Institute for Nanotechnology, Institute for Sustainability and Energy at Northwestern, Northwestern University, Evanston, Illinois 60208, United States;* orcid.org/0000-0003-3982-9812

Michael R. Wasielewski − *Department of Chemistry and International Institute for Nanotechnology, Institute for Sustainability and Energy at Northwestern, Northwestern University, Evanston, Illinois 60208, United States;* orcid.org/0000-0003-2920-5440

Complete contact information is available at: https://pubs.acs.org/10.1021/jacs.3c10232

Notes

The authors declare no competing financial interest.

■ ACKNOWLEDGMENTS

S.M.H., S.P., and A.L. acknowledge funding from the National Science Foundation Graduate Research Fellowship under Grant DGE-1842165. This work was supported by the National Science Foundation MSN #1808950. Work performed at the Center for Nanoscale Materials, a U.S. Department of Energy Office of Science User Facility, was supported by the U.S. DOE, Office of Basic Energy Sciences, under Contract No. DE-AC02-06CH11357. This work was supported by the U.S. Department of Energy, Office of Science, Office of Basic Energy Sciences under Award DE-FG02-99ER14999 (M.R.W.). J.T.H. gratefully acknowledges support from the U.S. Dept. of Energy, Office of Science, Basic Energy Science via grant no. DE-FG02-87ER13808. This work made use of the IMSERC NMR facility at Northwestern University, which has received support from the Soft and Hybrid Nanotechnology Experimental (SHyNE) Resource (NSF ECCS-1542205), Int. Institute of Nanotechnology, and Northwestern University. This work also made use of the EPIC facility of Northwestern University's NUANCE Center, which has received support from the Soft and Hybrid Nanotechnology Experimental (SHyNE) Resource (NSF ECCS-1542205), the MRSEC program (NSF DMR1720139) at the Materials Research Center, the International Institute for Nanotechnology (IIN), the Keck Foundation, and the State of Illinois, through the IIN. The authors would like to acknowledge Dr. Yuyang Wu for support with the temperature-dependent NMR experiments. Aspects of this work are adapted from the PhD dissertation of S.M.H.

■ REFERENCES

(1) Pietryga, J. M.; Park, Y.-S.; Lim, J.; Fidler, A. F.; Bae, W. K.; Brovelli, S.; Klimov, V. I. Spectroscopic and Device Aspects of Nanocrystal Quantum Dots. *Chem. Rev.* **2016**, *116* (18), 10513−10622.

(2) Hartley, C. L.; Kessler, M. L.; Dempsey, J. L. Molecular-Level Insight into Semiconductor Nanocrystal Surfaces. *J. Am. Chem. Soc.* **2021**, *143* (3), 1251−1266.

(3) Heuer-Jungemann, A.; Feliu, N.; Bakaimi, I.; Hamaly, M.; Alkilany, A.; Chakraborty, I.; Masood, A.; Casula, M. F.; Kostopoulou, A.; Oh, E.; Susumu, K.; Stewart, M. H.; Medintz, I. L.; Stratakis, E.; Parak, W. J.; Kanaras, A. G. The Role of Ligands in the Chemical Synthesis and Applications of Inorganic Nanoparticles. *Chem. Rev.* **2019**, *119* (8), 4819−4880.

(4) Harris, R. D.; Bettis Homan, S.; Kodaimati, M.; He, C.; Nepomnyashchii, A. B.; Swenson, N. K.; Lian, S.; Calzada, R.; Weiss, E. A. Electronic Processes within Quantum Dot-Molecule Complexes. *Chem. Rev.* **2016**, *116* (21), 12865−12919.

(5) Sun, P.; Xing, Z.; Li, Z.; Zhou, W. Recent Advances in Quantum Dots Photocatalysts. *Chem. Eng. J.* **2023**, *458*, No. 141399.

(6) Yuan, Y.; Jin, N.; Saghy, P.; Dube, L.; Zhu, H.; Chen, O. Quantum Dot Photocatalysts for Organic Transformations. *J. Phys. Chem. Lett.* **2021**, *12* (30), 7180−7193.

(7) Kamat, P. V. Quantum Dot Solar Cells. Semiconductor Nanocrystals as Light Harvesters. *J. Phys. Chem. C* **2008**, *112* (48), 18737−18753.

(8) Lin, S.; Peng, X. Current Status and Challenges of Solar Cells Based on Semiconductor Nanocrystals. *Energy Fuels* **2021**, *35* (23), 18928−18941.

(9) Stolle, C. J.; Harvey, T. B.; Korgel, B. A. Nanocrystal Photovoltaics: A Review of Recent Progress. *Nanotechnol. Sep. Eng.* **2013**, *2* (2), 160−167.

(10) Jang, E.; Jang, H. Review: Quantum Dot Light-Emitting Diodes. *Chem. Rev.* **2023**, *123* (8), 4663−4692.

(11) Nguyen, H. A.; Dixon, G.; Dou, F. Y.; Gallagher, S.; Gibbs, S.; Ladd, D. M.; Marino, E.; Ondry, J. C.; Shanahan, J. P.; Vasileiadou, E. S.; Barlow, S.; Gamelin, D. R.; Ginger, D. S.; Jonas, D. M.; Kanatzidis, M. G.; Marder, S. R.; Morton, D.; Murray, C. B.; Owen, J. S.; Talapin, D. V.; Toney, M. F.; Cossairt, B. M. Design Rules for Obtaining Narrow Luminescence from Semiconductors Made in Solution. *Chem. Rev.* **2023**, *123* (12), 7890−7952.

(12) Li, J.; Zhu, J.-J. Quantum Dots for Fluorescent Biosensing and Bio-Imaging Applications. *Analyst* **2013**, *138* (9), 2506−2515.

(13) Ahn, N.; Livache, C.; Pinchetti, V.; Klimov, V. I. Colloidal Semiconductor Nanocrystal Lasers and Laser Diodes. *Chem. Rev.* **2023**, *123* (13), 8251−8296.

(14) Park, Y.-S.; Roh, J.; Diroll, B. T.; Schaller, R. D.; Klimov, V. I. Colloidal Quantum Dot Lasers. *Nat. Rev. Mater.* **2021**, *6* (5), 382−401.

(15) Diroll, B. T.; Kirschner, M. S.; Guo, P.; Schaller, R. D. Optical and Physical Probing of Thermal Processes in Semiconductor and Plasmonic Nanocrystals. *Annu. Rev. Phys. Chem.* **2019**, *70* (1), 353−377.

(16) Akhavan, V. A.; Goodfellow, B. W.; Panthani, M. G.; Reid, D. K.; Hellebusch, D. J.; Adachi, T.; Korgel, B. A. Spray-Deposited $CuInSe_2$ Nanocrystal Photovoltaics. *Energy Environ. Sci.* **2010**, *3* (10), 1600−1606.

(17) Cohen, T. A.; Sharp, D.; Kluherz, K. T.; Chen, Y.; Munley, C.; Anderson, R. T.; Swanson, C. J.; De Yoreo, J. J.; Luscombe, C. K.; Majumdar, A.; Gamelin, D. R.; Mackenzie, J. D. Direct Patterning of Perovskite Nanocrystals on Nanophotonic Cavities with Electrohydrodynamic Inkjet Printing. *Nano Lett.* **2022**, *22* (14), 5681−5688.

(18) Hannah, D. C.; Gezelter, J. D.; Schaller, R. D.; Schatz, G. C. Reverse Non-Equilibrium Molecular Dynamics Demonstrate That Surface Passivation Controls Thermal Transport at Semiconductor−Solvent Interfaces. *ACS Nano* **2015**, *9* (6), 6278−6287.

(19) Harvey, S. M.; Houck, D. W.; Kirschner, M. S.; Flanders, N. C.; Brumberg, A.; Leonard, A. A.; Watkins, N. E.; Chen, L. X.; Dichtel, W. R.; Zhang, X.; Korgel, B. A.; Wasielewski, M. R.; Schaller, R. D.

Transient Lattice Response upon Photoexcitation in $CuInSe_2$ Nanocrystals with Organic or Inorganic Surface Passivation. *ACS Nano* **2020**, *14* (10), 13548−13556.

(20) Rowland, C. E.; Liu, W.; Hannah, D. C.; Chan, M. K. Y.; Talapin, D. V.; Schaller, R. D. Thermal Stability of Colloidal InP Nanocrystals: Small Inorganic Ligands Boost High-Temperature Photoluminescence. *ACS Nano* **2014**, *8* (1), 977−985.

(21) Hines, D. A.; Becker, M. A.; Kamat, P. V. Photoinduced Surface Oxidation and Its Effect on the Exciton Dynamics of CdSe Quantum Dots. *J. Phys. Chem. C* **2012**, *116* (24), 13452−13457.

(22) Morshedian, H.; Abolhasani, M. Accelerated Photostability Studies of Colloidal Quantum Dots. *Sol. RRL* **2023**, *7* (10), No. 2201119.

(23) Reichert, M. D.; Lin, C.-C.; Vela, J. How Robust Are Semiconductor Nanorods? Investigating the Stability and Chemical Decomposition Pathways of Photoactive Nanocrystals. *Chem. Mater.* **2014**, *26* (13), 3900−3908.

(24) Stolle, C. J.; Harvey, T. B.; Korgel, B. A. Photonic Curing of Ligand-Capped $CuInSe_2$ Nanocrystal Films. Proceedings of the 2014. *IEEE 40th Photovoltaic Specialist Conference (PVSC)*: Denver, June 8−13, 2004; IEEE: Piscataway, NJ, 2014; pp 270−274.

(25) Weidling, A. M.; Turkani, V. S.; Luo, B.; Schroder, K. A.; Swisher, S. L. Photonic Curing of Solution-Processed Oxide Semiconductors with Efficient Gate Absorbers and Minimal Substrate Heating for High-Performance Thin-Film Transistors. *ACS Omega* **2021**, *6* (27), 17323−17334.

(26) Han, H. S.; Choi, K. Y. Advances in Nanomaterial-Mediated Photothermal Cancer Therapies: Toward Clinical Applications. *Biomedicines* **2021**, *9* (3), 305.

(27) Hartley, C. L.; Dempsey, J. L. Electron-Promoted X-Type Ligand Displacement at CdSe Quantum Dot Surfaces. *Nano Lett.* **2019**, *19* (2), 1151−1157.

(28) Busby, E.; Anderson, N. C.; Owen, J. S.; Sfeir, M. Y. Effect of Surface Stoichiometry on Blinking and Hole Trapping Dynamics in CdSe Nanocrystals. *J. Phys. Chem. C* **2015**, *119* (49), 27797−27803.

(29) Krivenkov, V.; Samokhvalov, P.; Zvaigzne, M.; Martynov, I.; Chistyakov, A.; Nabiev, I. Ligand-Mediated Photobrightening and Photodarkening of CdSe/ZnS Quantum Dot Ensembles. *J. Phys. Chem. C* **2018**, *122* (27), 15761−15771.

(30) Shulenberger, K. E.; Keller, H. R.; Pellows, L. M.; Brown, N. L.; Dukovic, G. Photocharging of Colloidal CdS Nanocrystals. *J. Phys. Chem. C* **2021**, *125* (41), 22650−22659.

(31) Orfield, N. J.; Majumder, S.; Hu, Z.; Koh, F. Y.-C.; Htoon, H.; Hollingsworth, J. A. Kinetics and Thermodynamics of Killing a Quantum Dot. *ACS Appl. Mater. Interfaces* **2020**, *12* (27), 30695−30701.

(32) Orfield, N. J.; Majumder, S.; McBride, J. R.; Yik-Ching Koh, F.; Singh, A.; Bouquin, S. J.; Casson, J. L.; Johnson, A. D.; Sun, L.; Li, X.; Shih, C.-K.; Rosenthal, S. J.; Hollingsworth, J. A.; Htoon, H. Photophysics of Thermally-Assisted Photobleaching in "Giant" Quantum Dots Revealed in Single Nanocrystals. *ACS Nano* **2018**, *12* (5), 4206−4217.

(33) Hens, Z.; Martins, J. C. A Solution NMR Toolbox for Characterizing the Surface Chemistry of Colloidal Nanocrystals. *Chem. Mater.* **2013**, *25* (8), 1211−1221.

(34) Flamee, S.; Cirillo, M.; Abe, S.; De Nolf, K.; Gomes, R.; Aubert, T.; Hens, Z. Fast, High Yield, and High Solid Loading Synthesis of Metal Selenide Nanocrystals. *Chem. Mater.* **2013**, *25* (12), 2476−2483.

(35) Anderson, N. C.; Hendricks, M. P.; Choi, J. J.; Owen, J. S. Ligand Exchange and the Stoichiometry of Metal Chalcogenide Nanocrystals: Spectroscopic Observation of Facile Metal-Carboxylate Displacement and Binding. *J. Am. Chem. Soc.* **2013**, *135* (49), 18536−18548.

(36) Singh, S.; Leemans, J.; Zaccaria, F.; Infante, I.; Hens, Z. Ligand Adsorption Energy and the Postpurification Surface Chemistry of Colloidal Metal Chalcogenide Nanocrystals. *Chem. Mater.* **2021**, *33* (8), 2796−2803.

(37) Hassinen, A.; Moreels, I.; De Nolf, K.; Smet, P. F.; Martins, J. C.; Hens, Z. Short-Chain Alcohols Strip X-Type Ligands and Quench the Luminescence of PbSe and CdSe Quantum Dots, Acetonitrile Does Not. *J. Am. Chem. Soc.* **2012**, *134* (51), 20705−20712.

(38) Anderson, N. C.; Owen, J. S. Soluble, Chloride-Terminated CdSe Nanocrystals: Ligand Exchange Monitored by 1H and 31P NMR Spectroscopy. *Chem. Mater.* **2013**, *25* (1), 69−76.

(39) Hannah, D. C.; Dunn, N. J.; Ithurria, S.; Talapin, D. V.; Chen, L. X.; Pelton, M.; Schatz, G. C.; Schaller, R. D. Observation of Size-Dependent Thermalization in CdSe Nanocrystals Using Time-Resolved Photoluminescence Spectroscopy. *Phys. Rev. Lett.* **2011**, *107* (17), No. 177403.

(40) Tamulaitis, G. Origin of Carrier Heating in Semiconductor Nanocrystals: Excess Energy of Photoexcited Electrons or Auger Processes? *J. Phys.: Condens. Matter* **1998**, *10* (45), 10307.

(41) Kirschner, M. S.; Diroll, B. T.; Guo, P.; Harvey, S. M.; Helweh, W.; Flanders, N. C.; Brumberg, A.; Watkins, N. E.; Leonard, A. A.; Evans, A. M.; Wasielewski, M. R.; Dichtel, W. R.; Zhang, X.; Chen, L. X.; Schaller, R. D. Photoinduced, Reversible Phase Transitions in All-Inorganic Perovskite Nanocrystals. *Nat. Commun.* **2019**, *10* (1), 504.

(42) Drijvers, E.; De Roo, J.; Martins, J. C.; Infante, I.; Hens, Z. Ligand Displacement Exposes Binding Site Heterogeneity on CdSe Nanocrystal Surfaces. *Chem. Mater.* **2018**, *30* (3), 1178−1186.

(43) Dümbgen, K. C.; Infante, I.; Hens, Z. Localizing Oleylamine Ligands on Amine−Halide Copassivated Indium Phosphide Nanocrystals. *Chem. Mater.* **2023**, *35* (11), 4393−4403.

(44) Dou, F. Y.; Harvey, S. M.; Mason, K. G.; Homer, M. K.; Gamelin, D. R.; Cossairt, B. M. Effect of a Redox-Mediating Ligand Shell on Photocatalysis by CdS Quantum Dots. *J. Chem. Phys.* **2023**, *158* (18), 184705.

(45) Homer, M. K.; Kuo, D.-Y.; Dou, F. Y.; Cossairt, B. M. Photoinduced Charge Transfer from Quantum Dots Measured by Cyclic Voltammetry. *J. Am. Chem. Soc.* **2022**, *144* (31), 14226−14234.

(46) Morris-Cohen, A. J.; Vasilenko, V.; Amin, V. A.; Reuter, M. G.; Weiss, E. A. Model for Adsorption of Ligands to Colloidal Quantum Dots with Concentration-Dependent Surface Structure. *ACS Nano* **2012**, *6* (1), 557−565.

(47) Fragata, M.; Viruvuru, V.; Dudekula, S. Theoretical Consideration of the Use of a Langmuir Adsorption Isotherm To Describe the Effect of Light Intensity on Electron Transfer in Photosystem II. *J. Phys. Chem. B* **2007**, *111* (12), 3315−3320.

(48) Tran, V. A.; Lee, S.-W. pH-Triggered Degradation and Release of Doxorubicin from Zeolitic Imidazolate Framework-8 (ZIF8) Decorated with Polyacrylic Acid. *RSC Adv.* **2021**, *11* (16), 9222−9234.

(49) Owen, J. The Coordination Chemistry of Nanocrystal Surfaces. *Science* **2015**, *347* (6222), 615−616.

(50) Knauf, R. R.; Lennox, J. C.; Dempsey, J. L. Quantifying Ligand Exchange Reactions at CdSe Nanocrystal Surfaces. *Chem. Mater.* **2016**, *28* (13), 4762−4770.

(51) Oka, K.; Shibue, T.; Sugimura, N.; Watabe, Y.; Winther-Jensen, B.; Nishide, H. Long-Lived Water Clusters in Hydrophobic Solvents Investigated by Standard NMR Techniques. *Sci. Rep.* **2019**, *9* (1), 223.

(52) Nakahara, M.; Wakai, C. Monomeric and Cluster States of Water Molecules in Organic Solvent. *Chem. Lett.* **1992**, *21* (5), 809−812.

(53) Chen, J. Y.-C.; Martí, A. A.; Turro, N. J.; Komatsu, K.; Murata, Y.; Lawler, R. G. Comparative NMR Properties of H_2 and HD in Toluene-d_8 and in H_2/HD@C60. *J. Phys. Chem. B* **2010**, *114* (45), 14689−14695.

(54) Kuehnel, M. F.; Wakerley, D. W.; Orchard, K. L.; Reisner, E. Photocatalytic Formic Acid Conversion on CdS Nanocrystals with Controllable Selectivity for H_2 or CO. *Angew. Chem., Int. Ed.* **2015**, *54* (33), 9627−9631.

(55) Aslan, E.; Birinci, O.; Aljabour, A.; Özel, F.; Akın, I.; Hatay Patir, I.; Kus, M.; Ersoz, M. Photocatalytic Hydrogen Evolution by Oleic Acid-Capped CdS, CdSe, and $CdS_{0.75}Se_{0.25}$ Alloy Nanocrystals. *ChemPhysChem* **2014**, *15* (13), 2668−2671.

https://doi.org/10.1021/jacs.3c10232
J. Am. Chem. Soc. XXXX, XXX, XXX−XXX

(56) Fritzinger, B.; Capek, R. K.; Lambert, K.; Martins, J. C.; Hens, Z. Utilizing Self-Exchange To Address the Binding of Carboxylic Acid Ligands to CdSe Quantum Dots. *J. Am. Chem. Soc.* **2010**, *132* (29), 10195−10201.

(57) Lee, S. F.; Osborne, M. A. Photodynamics of a Single Quantum Dot: Fluorescence Activation, Enhancement, Intermittency, and Decay. *J. Am. Chem. Soc.* **2007**, *129* (29), 8936−8937.

(58) Lee, S. F.; Osborne, M. A. Brightening, Blinking, Bluing and Bleaching in the Life of a Quantum Dot: Friend or Foe? *ChemPhysChem* **2009**, *10* (13), 2174−2191.

https://doi.org/10.1021/jacs.3c10232
J. Am. Chem. Soc. XXXX, XXX, XXX−XXX